Mutations in KARS cause a severe neurological and neurosensory disease with optic neuropathy

Sophie Scheidecker, Séverine Bär, Corinne Stoetzel, Véronique Geoffroy, Béatrice Lannes, Bruno Rinaldi, Frédéric Fischer, Hubert D. Becker, Valérie Pelletier, Cécile Pagan, et al.

Sylvie Friant ORCID iD: 0000-0002-5412-6288

May 2019 Human Mutation DOI: 10.1002/humu.23799

Mutations in *KARS* cause a severe neurological and neurosensory disease with optic neuropathy

Sophie Scheidecker[1,2]*, Séverine Bär[3]*, Corinne Stoetzel[1]*, Véronique Geoffroy[1], Béatrice Lannes[4], Bruno Rinaldi[3], Frédéric Fischer[3], Hubert D. Becker[3], Valérie Pelletier[5], Cécile Pagan[6], Cécile Acquaviva-Bourdain[6], Stéphane Kremer[7], Marc Mirande[8], Christine Tranchant[9], Jean Muller[1,2], Sylvie Friant[2]§, Hélène Dollfus[1,5]§

1. Laboratoire de Génétique Médicale, INSERM U1112, Institut de Génétique Médicale d'Alsace, Université de Strasbourg, Strasbourg, France

2. Laboratoires de Diagnostic Génétique, Hôpitaux Universitaires de Strasbourg, Strasbourg, France

3. Laboratoire de Génétique Moléculaire, Génomique, Microbiologie (GMGM), UMR7156, Université de Strasbourg, CNRS, Strasbourg, France

4. Service d'Anatomo-pathologie, Hôpitaux Universitaires de Strasbourg, Hôpital de Hautepierre, Strasbourg, France

5. Centre de Référence pour les affections rares en génétique ophtalmologique, CARGO, Filière SENSGENE, Hôpitaux Universitaires de Strasbourg, Strasbourg, France

6. Service de Biochimie et Biologie Moléculaire, Centre de Biologie et de Pathologie Est, Hospices Civils de Lyon, Lyon, France

7. Service de Neuroradiologie/Imagerie 2, CHU de Strasbourg, Hôpital de Hautepierre, Strasbourg, France

8. Institute for Integrative Biology of the Cell (I2BC), CEA, CNRS, Univ. Paris-Sud, Université Paris-Saclay, Gif-sur-Yvette, France

9. Service de Neurologie Hôpitaux Universitaires de Strasbourg, Hôpital de Hautepierre, Strasbourg, France

* These authors contributed equally and should be considered joint first author.

§ These authors contributed equally and should be considered joint last author.

Corresponding author:

Email address: s.friant@unistra.fr

Laboratoire de Génétique Moléculaire, Génomique, Microbiologie (GMGM), UMR7156, Université de Strasbourg, CNRS, Strasbourg, France

Correspondence:

Sylvie Friant, GMGM, UMR7156, 21 rue Descartes, 67000 Strasbourg, France. Email: s.friant@unistra.fr

Hélène Dollfus, LGM, INSERM U1112, Faculté de Médecine, Batiment3, 11 rue Humann, 67085 Strasbourg cedex, France. Email : dollfus@unistra.fr

Funding information:

Contract grant sponsors: Hôpitaux Universitaires de Strasbourg (Strasbourg, France) API 2013-2014 HUS N° 5885 (to SS and HD), CNRS (to SF), INSERM (to HD and SB), Université de Strasbourg (HD, SF, FF, HDB and IDEX 2015 Attractivité to SB), the French National Program Investissement d'Avenir administered by the Agence National de la Recherche (ANR) MitoCross Laboratory of Excellence (Labex) funded

as ANR-10-IDEX-0002-02 (to FF and HDB) ; whole exome sequencing was performed by IntegraGen platform, Evry, France.

Abstract

Mutations in genes encoding aaRSs (aminoacyl-tRNA synthetases) have been reported in several neurological disorders. KARS is a dual localized lysyl-tRNA synthetase (LysRS) and its cytosolic isoform belongs to the multiple aminoacyl-tRNA synthetase complex (MSC). Biallelic mutations in *KARS* gene were described in a wide phenotypic spectrum ranging from non-syndromic deafness to complex impairments. Here, we report on a patient with severe neurological and neurosensory disease investigated by whole exome sequencing and found to carry biallelic mutations c.683C>T (p.Pro228Leu) and c.871T>G (p.Phe291Val), the second one being novel, in the *KARS* gene. The patient presented with an atypical clinical presentation with an optic neuropathy not previously reported. At the cellular level, we show that cytoplasmic KARS was expressed at a lower level in patient cells and displayed decreased interaction with MSC. In vitro, these two KARS variants have a decreased aminoacylation activity compared to wild type KARS, the p.Pro228Leu being the most affected. Our data suggest that dysfunction of cytoplasmic KARS resulted in decreased level of translation of the nuclear encoded lysine rich proteins belonging to the respiratory chain complex, thus impairing mitochondria functions.

Graphical Abstract

Here, we report on a patient with severe neurological disease, found to carry biallelic mutations c.683C>T (p.Pro228Leu) and c.871T>G (p.Phe291Val) in the lysyl-tRNA synthetase KARS.

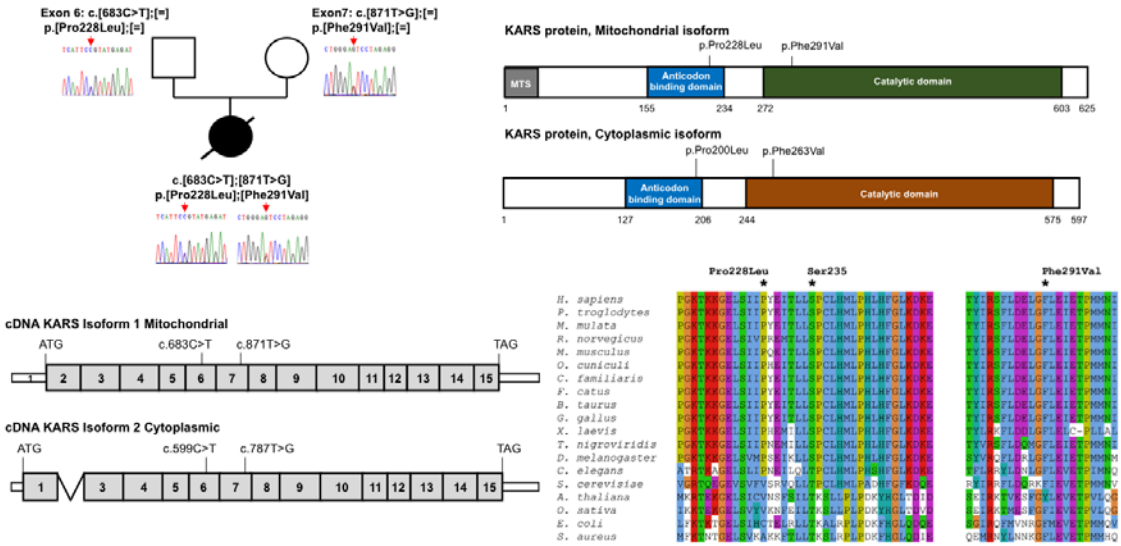

Key words

lysyl-tRNA synthetase, translation, aaRS, neurological disorder, optic neuropathy, deafness, mitochondrial respiratory chain defect

Introduction

Aminoacyl-tRNA synthetases (aaRS) belong to a ubiquitously expressed group of enzymes responsible for aminoacylation, the process of attaching amino acids to their cognate tRNA. In humans, 37 aaRS proteins are encoded by nuclear genes. These enzymes can be divided into 3 groups according to the cellular compartment where the aminoacylation is performed: cytoplasm, mitochondria or both. KARS is one of the 3 human aaRS with a dual localization and its cytosolic isoform is a component of

a multiple aminoacyl-tRNA synthetase complex (MSC) (Havrylenko & Mirande, 2015). This complex increases the efficiency of protein synthesis and is composed of at least nine aaRS and three accessory proteins (p18, p38 and p43). The p38/AIMP2 scaffold protein serves as a cytoplasmic anchor to retain KARS in the complex (Kaminska et al., 2009; Quevillon et al., 1999). The phosphorylation at the serine in position 207 (P-S207) of the KARS protein induces its release from the MSC and its translocation into the nucleus for non-canonical activities in transcription (Debard et al., 2017; Ofir-Birin et al., 2013). The P-S207 KARS leads also to increased levels of diadenosine tetraphosphate (Ap4A), a second messenger acting as a positive regulator of the microphthalmia-associated transcription factor (MITF) (Lee, Nechushtan, Figov, & Razin, 2004). Interestingly, increased levels of Ap4A were observed in tears of patients with dry eye and with congenital aniridia (Peral et al., 2006; Peral et al., 2015), and in the aqueous humour from patients with primary open-angle glaucoma (Castany et al., 2011).

Mutations in genes encoding aaRS are reported in a wide spectrum of inherited human disorders (Antonellis & Green, 2008; Sauter et al., 2015). Mutations in genes encoding mitochondrial aaRS are associated with autosomal recessive isolated or syndromic phenotypes involving tissues with high metabolic needs such as brain, muscle, heart, and liver (Gotz et al., 2011; Sofou et al., 2015). Mutations in genes encoding cytoplasmic aaRS are implicated in different disorders, including neurological diseases, with autosomal recessive or dominant inheritance (Latour et al., 2010). Mutations in the *KARS* gene (MIM# 601421), encoding the lysyl-tRNA synthetase, were described initially in peripheral neuropathy (McLaughlin et al., 2010) and few years later in non syndromic hearing loss (Santos-Cortez et al., 2013). A wide range of clinical features was reported in patients carrying biallelic mutations in *KARS*

including phenotypes suggesting mitochondrial disorder (Kohda et al., 2016; Lieber et al., 2013; McMillan et al., 2015; Murray et al., 2017; Verrigni et al., 2017; Zhou et al., 2017).

Here, we report a patient, with biallelic variants in *KARS* identified by whole exome sequencing, who presented with severe neurological and neurosensory impairment. Interestingly, while in the patient's fibroblasts the expression of the mitochondrial isoform of the protein was slightly increased, a reduced activity of the complexes I and IV was observed in the patient's skeletal muscle which is compatible with a mitochondrial disorder. Although this first result seemed contradictory, we questioned whether the dysfunction of the patient's respiratory chain could be related to a decreased expression of some members of complex I and IV encoded by the nuclear genome, thus translated into the cytoplasm and afterwards imported into the mitochondria. Indeed, a lower amount of the cytoplasmic isoform of KARS was observed in the patient's cells. At the molecular level, using a yeast two-hybrid interaction assay, we observed a decreased interaction between KARS bearing either of the patient mutations and p38, the interaction partner of KARS in the MSC complex. The association of KARS into the MSC complex controls its canonical function in translation from those non-canonical as the regulation of transcription.

This study suggests that a dysfunction in cytoplasmic KARS due to the patient's missense mutations decreased the efficiency of translation of the nuclear encoded lysine rich proteins belonging to respiratory chain complexes, thus impairing mitochondria functions.

Materials and Methods

Standard protocol approvals and patient consents

After informed consent of the patient and her parents according to the French legislation, peripheral blood samples were obtained from the affected individual and her parents as well as control individuals. DNA from all collected samples was extracted according to standard procedures. The objectives and the aim of the study were clearly explained to the patient and this study was approved by the local ethics committee at Hôpitaux Universitaires de Strasbourg (Strasbourg University Hospital).

Mutational analysis

Whole exome sequencing was performed in the affected individual (II-1) and the healthy parents (I-1 and I-2). Exons of DNA samples were captured with in-solution enrichment methodology (Agilent SureSelect XT Clinical Research Exome – 54 Mb) and paired-end 75 bases massively parallel sequencing was performed on Illumina HiSeq. 4000 instrument. SNP and INDEL variant calling were performed with CASAVA1.8.2.

Exome data processing, variant calling and variant annotation were performed using VaRank (Geoffroy et al., 2015). We excluded variants present in dbSNP144 and annotated as non-pathogenic (using the "ClinicalSignificance" field) validated by at least 2 methods (using the "Validation Status" field) and variants with an allele frequency of more than 1% in the dbSNP database (Sherry et al., 2001), the Exome Variant Server (http://evs.gs.washington.edu/EVS/), the 1000Genomes (Genomes Project et al., 2015), the ExAC Browser database (Lek et al., 2016) or our internal exome database. Variant effect on the nearest splice site was predicted using

MaxEntScan (Yeo & Burge, 2004), NNSplice (Reese et al., 1997) and Splice Site Finder (based on (Shapiro & Senapathy, 1987)). Structural variants were predicted using CANOES (Backenroth et al., 2014) and annotated by AnnotSV (Geoffroy et al., 2018). We focused on variants consistent with an autosomal recessive inheritance (patient compound heterozygous or homozygous).

The mutations were confirmed by bidirectional Sanger sequencing of purified polymerase chain reaction (PCR) products, performed by the GATC Sequencing Facilities (Konstanz, Germany). The PCR primers are summarized in Supp. Table S1.

Enzymatic analyses

Enzymatic activities of the mitochondrial respiratory chain complexes were measured in muscle as reported previously (Bourges et al., 2004).

The *in vitro* aminoacylation analyses were done as previously described, by using [^{3}H]-labeled lysine (PerkinElmer Life Sciences, 1 mCi/ml) (Francin et al., 2002).

RNA extraction, cDNA synthesis

RNA was extracted from primary skin fibroblasts of the patient and a healthy unrelated control using RNeasy RNA kit (Qiagen). Then we performed reverse transcription of mRNA using the BioRad iScriptTM cDNA Synthesis Kit (BioRad). Primers used are summarized in Supp. Table S1.

Western blot and immunofluorescence of human primary cells

Primary skin fibroblasts from the patient and control individuals were grown in DMEM supplemented with 10% fetal calf serum (FCS) and 1% Penicillin-streptomycin-glutamin (PSG). Cycloheximide (CHX) pulse chase experiments were

done to analyse the stability of the proteins (Kao et al., 2015). Cells were collected at different time points (0, 1, 4 and 8 hours) after cycloheximide (Sigma, C7698) addition into the cell medium at a final concentration of 100 mg/L. Cells were collected in RIPA buffer for western blot and KARS detected with three primary antibodies (Kaminska et al., 2007): IgG anti-ΔNter-KARS (polyclonal directed against the catalytic domain of the KARS), IgG anti-cytoKARS (polyclonal directed against a peptide in the N-terminal part of the cytoplasmic form) and IgG anti-mitoKARS (polyclonal directed against a peptide in the N-terminal part of the mitochondrial form). Cox4 (Abcam AB14744), Cox2 (Invitrogen 459150) and Grim19 (Santa Cruz SC66195) were detected with mouse monoclonal antibodies, NDUFB6 (Abcam 103531) with a rabbit polyclonal antibody. Quantification of bands in western blot was done using ImageLab (BioRad) and the stainfree system after inclusion of 0.5% (v/v) 2,2,2-Trichloroethanol (TCE, Sigma T54801) into the polyacrylamide gel and revelation by UV of the fluorescent tryptophan residues of the proteins to determine total amount of proteins on the membrane (Ladner et al., 2004).

For immunofluorescence, cells were first incubated with 200 nM Mitotracker red (Thermofisher Scientific, M22425), then fixed with 4% formaldehyde and permeabilised with 0,5% triton. After blocking with phosphate-buffered saline (PBS) 20% FCS, the cells were incubated for 1 hr with the primary antibody (Rabbit mAb to KARS, Abcam, ab129080), washed 3 times in PBS, incubated for 1 hr with secondary antibody (goat anti-rabbit Alexa Fluor 488 IgG, Invitrogen, A-11008) and DAPI, washed again in PBS and mounted in Elvanol No-Fade™ mounting medium. Observation was done on a Zeiss Axio Observer D1, 400X magnification.

KARS and p38 interaction assays by yeast two-hybrid

The pEG202 (LexA DNA-binding protein fusion, HIS3) or pJG4-5 (*GAL1* minimal promoter bearing the transcription activation domain, TRP1) yeast two-hybrid vectors bearing the p38 or cytoplasmic KARS (protein size 597 aa) cDNA were used in this study (Quevillon et al., 1999). The P200L or F263V mutation was introduced into the cytoplasmic KARS cDNA by PCR with Phusion High-Fidelity DNA polymerase (Thermo Scientific). The plasmids pSF496 (pEG202-KARS-P200L), pSF497 (pJG4-5-KARS-P200L), pSF498 (pEG202-KARS-F263V) and pSF499 (pJG4-5-KARS-F263V) sequences were verified (GATC Biotech). The *Saccharomyces cerevisiae* EGY48 (*MAT α ura3 his3 trp1 LexAop(x6)LEU2*) two-hybrid strain bearing the pSH18-34 (LacZ reporter plasmid; LexAop(x8)-LacZ, URA3) plasmid was used. Yeast cells were transformed by the indicated plasmids and two-hybrid assays were done as described (Golemis et al., 2001). The β-galactosidase activity resulting from LacZ gene expression was monitored by ONPG (O-nitrophenyl-beta-D-galactopyranoside) assay (Gietz et al., 1997).

KARS and p38 interaction assays by coimmunoprecipitation (coIP)

Cells were grown in DMEM (Gibco Invitrogen, 31885), 10% of FBS and Penicillin and Streptomycin (P/S) to full confluence. Cells were rinsed with PBS at 4°C, resuspended in non-denaturing lysis buffer (20 mM Tris HCL pH 8; 137 mM NaCl; 1% Nonidet P-40; 2 mM EDTA) with a protease inhibitor cocktail (Roche 06538282001) and incubated on ice for 15 min under gentle shaking. The samples were then centrifuged at 12,000X g for 20 min at 4°C, protein concentration was measured using Qubit® Protein Assay Kit (Life Technologies) and then used for immunoprecipitation. 500µg of cell lysate were incubated with KARS antibodies

(polyclonal rabbit, (Kaminska et al., 2007)) or with p38 antibodies (polyclonal rabbit, (Mirande et al., 1982)) on a rocker shaker overnight at 4°C. The immunocomplexes were captured by adding protein G sepharose beads (DUTSCHER 17-0618-05) for 2 h at 4°C under gentle shaking. Sepharose G beads were washed 6 times for 5 min with the non-denaturing lysis buffer bearing protease inhibitor cocktail, then resuspended in 2X Laemmli buffer and boiled for 10 min at 95°C to dissociate the immunocomplexes from the beads, prior analysis by western-blot. Actin B (ACTB, antibodies from Novus NB600-501SS) was used as a negative control for the coIP and as loading control for the Input.

Results

Clinical report of a patient

The female patient, born after an unremarkable pregnancy, was the only child of unrelated parents. She had history of motor development delays due to cerebellar ataxia. She attended normal schooling. Bilateral congenital deafness was diagnosed during the first year at school. Cerebral RMN scan performed at the age of 10 was unremarkable.

The clinical manifestations were stable until the age of 28, when she developed additional clinical features with progressive visual impairment. The visual acuity was measured at 1.30 LogMAR. Fundus examination showed no retinal involvement, but reduced thickness in the temporal region (Figure 1A). Goldman visual fields showed concentric decrease of peripheral isopters. The visual acuity worsened significantly the years later. Cerebellar syndrome increased progressively and other neurological features were observed with a pyramidal syndrome of the 4 limbs, a dystonia, and pseudobulbar syndrome. The metabolic screen showed hyperlactatemia. The cerebral

RMN scan performed at 28 years old revealed white matter anomalies of the dentate nucleus, optic radiations and of the corpus callosum splenium (Figure 1B). Electromyography showed a sensitive axonal polyneuropathy of the lower limbs.

In the hypothesis of a mitochondrial disorder a muscle biopsy was performed which showed microscopic features compatible with a mitochondriopathy with no ragged-red fibers but numerous COX negative fibers (Figure 2A). The study of enzymatic complex of the mitochondrial respiratory chain in the skeletal muscle revealed a partial deficit in the complexes I (68 %) and IV activities (62 %) (Figure 2B). The study of the mitochondrial DNA, including the research of the 3 main mutations, the analysis of the deletion and the sequencing of the 22 tRNA, was normal.

This clinical presentation worsened with a progressive cognitive decline and the patient died at the age of 33.

Whole exome sequencing identified biallelic mutations in the *KARS* gene of the patient.

In the absence of a molecular diagnosis, we performed whole exome sequencing for the patient and her healthy parents. In the proband's sample, 105.423 genetics variants (SNV + Indel) were identified. Bioinformatics analyses narrowed down the number of variants to biallelic variants in 5 genes (Supp. Table S2). We focused on two biallelic variations (NM_001130089.1: c.683C>T, p.Pro228Leu and c.871T>G, p.Phe291Val) in the *KARS* gene (Figure 3). Sanger sequencing confirmed the mutations and familial segregation analysis was consistent with disease transmission (Figure 3A). The c.683C>T mutation was previously reported in a patient suspected with a mitochondrial disorder (Lieber et al., 2013). The c.871T>G mutation is absent from dbSNP, 1000 Genomes, EVS, exAC database and our internal database. This variant

was localized in the catalytic domain of the KARS protein (Figure 3) and was predicted to be deleterious according to SIFT (Kumar et al., 2009) and PolyPhen-2 (Adzhubei et al., 2010). The amino acid Phe291 is conserved from metazoan to bacteria (*E. coli* and *S. aureus*), with the exception of the plant *Arabidopsis thaliana*, and the Pro228 is conserved across metazoan species but not in plant, fungi or in bacteria (Figure 3D).

The mRNA coding for the cytoplasmic and mitochondrial isoforms of KARS are present in the fibroblasts of the patient.

The difference between the two isoforms of KARS is due to alternative splicing, with splicing of exon 1 to exon 3 for the cytoplasmic isoform, whereas the mitochondrial isoform includes exon 2 (Figure 3B). To determine whether both isoforms of KARS were present, the cDNA obtained after reverse transcription of RNAs extracted from skin fibroblast of the patient was analyzed by PCR. Using primers from exon 1 to exon 4 and exon 2 to exon 3, we observed the two isoforms in the patient and in a healthy control. Moreover, exons 5 to 9 were analyzed by sequencing and the two mutations were detected in the cDNA of the patient (Figure 4A). We did not observe a splicing effect of the two mutations.

Quantification of KARS mRNA by q-RT-PCR revealed a significant increase of mitochondrial KARS in the patient cells compared to the control, whereas no difference was observed in the expression of cytoplasmic KARS (Figure 4B).

KARS protein level is decreased in the cytoplasm of patient fibroblasts

The mitochondria and cytoplasmic isoforms of KARS differ by their N-terminal part (Figure 3C). We observed differences at the mRNA levels indicating an increase of

mitochondrial KARS in the patient cells compared to control cells (Figure 4B), therefore KARS protein level was analyzed in the patient cells. Patient and control fibroblasts were grown in complete medium and total proteins collected for western blotting. KARS was detected with antibodies directed either against the catalytic domain, thus recognizing mitochondrial and cytoplasmic isoforms or specifically against the N-terminal thus specific for each isoform (Figure 4C, Supp. Figure S1). The overall expression of KARS is lower in patient cells and this is due to a decrease in the cytoplasmic KARS. The level of mitochondrial KARS is only slightly higher in patient cells, which correlates with what was observed at the mRNA level (Figure 4). This decrease in the cytoplasmic form of KARS was not detected to that extent at the mRNA level, this could be due to a higher degradation or decreased stability of the KARS-P200L and/or KARS-F263V proteins bearing the patient mutation compared to the wild type protein. This result was confirmed by analyzing the stability of the total KARS proteins after cycloheximide treatment to inhibit de novo protein synthesis (Figure 4D). Immunofluorescence with cytoplasmic KARS antibodies and Mitotracker red staining done on fibroblasts revealed no differences in the mitochondria staining between the control and the patient cells (Figure 5). The KARS signal was very faint in the patient cells (affected) indicating a lower level of cytoplasmic KARS compared to the control (ctrl) cells (Figure 5).

The KARS-P200L and KARS-F263V mutations impair KARS association to the multiple aminoacyl-tRNA synthetase (MSC) complex

In human cells, the aaRS are organized in a multiple aminoacyl-tRNA synthetase (MSC) complex (Havrylenko & Mirande, 2015). p38, a core protein responsible for assembly of the MSC complex, directly interacts with KARS (Ofir-Birin et al., 2013; Quevillon et al., 1999). To better understand the cellular defects linked to the two

disease mutations in KARS, we studied their interaction with p38 by yeast two-hybrid assays. EGY48 yeast cells were transformed by pEG202 plasmid expressing p38, KARS, KARS-P200L or KARS-F263V cDNA, the different LexA DNA-binding protein fusions do not activate transcription and expression of the LexA fusions was confirmed by the repression assay (Figure 6A) (Golemis et al., 2001). These results show that the P200L or F263V mutation did not impair the production of the KARS protein. The lack of DNA-binding activity by the p38, KARS, KARS-P200L or KARS-F263V protein in fusion with the *GAL1* promoter transcriptional activation domain cloned in pJG4-5 plasmid was also confirmed (Figure 6A) (Golemis et al., 2001). The yeast two-hybrid assay was done to determine the interaction between p38 and KARS, KARS-P200L or KARS-F263V proteins. As previously described, p38 and KARS display a strong interaction in both combinations of two-hybrid plasmids (Quevillon et al., 1999), measured by the ONPG assay to determine the level of *lacZ* transcription (Figure 6B). The β-galactosidase produced by the *lacZ* reporter for two-hybrid interaction cleaves the colorless ONPG substrate in galactose and o-nitrophenol (ONP) that absorbs at 420 nm. The KARS-P200L and KARS-F263V mutants display a statistically significant reduced interaction with p38 compared to wild-type KARS (Figure 6B). The Pro200 (Pro228 in the mitochondrial KARS) residue is in the anticodon-binding domain of KARS close to the Ser207 (Ser235 mitoKARS) phosphorylation site essential for p38 interaction (Ofir-Birin et al., 2013) (Figure 3E). The Phe263 (Phe291 mitoKARS) is at the KARS-p38 interaction interface (Figure 3E). These yeast two-hybrid data were confirmed by coimmunoprecipitation (Co-IP) analyses done on protein lysates extracted from patient and control fibroblasts (Figure 6C). The levels of KARS and p38 proteins were lower in the protein lysate (Input) of the patient cells compared to the control.

However after immunoprecipitation (IP) of either KARS or p38, these two proteins were highly enriched in the IP fractions (Figure 6C), but the interacting protein was observed in the control samples and only barely detectable in the patient Co-IP samples (Figure 6C).

These different results show that KARS-P200L and KARS-F263V mutations might be pathogenic due to their reduced p38 binding, impairing the association of the cytoplasmic KARS Lysine-tRNA synthetase with the MSC complex and affecting its function in cytoplasmic protein synthesis.

The two patient variants are affected in aminoacylation *in vitro* and the level of lysine-rich COX4 and NDUFB6 mitochondrial protein is decreased in patient fibroblasts

To determine the aminoacylation activity, wild-type KARS and the two patient variants KARS-P200L or KARS-F263V were produced as recombinant proteins in *E. coli* and purified (Supp. Figure S3). A time course of aminoacylation was conducted and the relative aminoacylation activity was determined (Figure 7A). The KARS-P200L shows a strong decrease in its relative activity compared to wild type KARS with only 0.14, and the KARS-F263V displays a two-fold decrease with 0.49 of relative activity (Figure 7A). This indicates that *in vitro* these two variants are affected in their aminoacylation level compared to wild-type KARS.

A decreased activity of complex I and IV of the respiratory chain was observed in the patient skeletal muscle (Figure 2B), there was an overexpression of mitochondrial KARS in patient cells (Figure 4), and the cytoplasmic KARS-P200L or KARS-F263V patient proteins interacted poorly with the MSC complex and are affected in protein synthesis activity (Figures 6 and 7A). Therefore, we wondered whether the altered

mitochondria function could be due to lower levels of lysine rich members of complex I and IV encoded by the nuclear genome and thus translated in the cytoplasm before being imported into the mitochondria. Indeed, the cytoplasmic form of the mutated KARS seems to be affected with a decreased protein level and impaired association to the MSC complex (Figures 4, 5 and 6). To verify this hypothesis, we determined which members of complex I and IV were rich in lysine (Supp. Figure S2A) and among these we analyzed the protein level of the nuclearly encoded COX4 (11.8% of lysine) and NDUFB6 (10,9% of lysine), as well as the nuclearly encoded GRIM19 with less lysine (4.2%), and COX2 (1.8% of lysine) encoded by the mitochondrial genome (Figure 7B). The western blot of total protein extracts from control and patient cells shows that the protein levels of COX4 and NDUFB6 but not GRIM19 and COX2 were decreased in the patient fibroblast (Figure 7B and Supp. Figure S2B). This indicates that the mitochondrial dysfunction observed in the patient skeletal muscle may indeed be due to defects in the cytoplasmic KARS, leading to a lower synthesis of lysine-rich nuclearly encoded complex I and IV proteins.

Discussion

The lysyl tRNA synthetase *KARS* is one of the 37 aa tRNA synthetase genes and one of the three dual localized aaRS. A single gene encodes these dual localized aaRS, whereas mitochondrial aaRSs are encoded in the nucleus by a specific gene different from those coding for the cytosolic aaRSs (Bonnefond et al., 2005). The two mRNAs of KARS are transcribed by an alternative splicing and are translated in the cytoplasm to form the cytoplasmic isoform and the precursor of the mitochondrial isoform bearing the MTS (mitochondria targeting sequence) (Figure 3). The mature form of mitochondrial KARS is produced during mitochondrial import by cleavage of the N-terminal MTS of the precursor (Dias et al., 2012). The cytoplasmic isoform represents

approximately 70% and the mitochondrial isoform about 30 % of the mature transcript from the *KARS* gene (Tolkunova, Park, Xia, King, & Davidson, 2000).

A mitochondrial defect phenotype associated with *KARS* mutations

Mitochondrial disorders comprise a heterogeneous group of diseases due to mitochondrial dysfunctions that can have pleiotropic effects. The features can include leukoencephalopathy, sensorineural deafness, optic atrophy, and ataxia. Less than 15-30 % of suspected mitochondrial disorders are due to a mitochondrial DNA anomaly (Dimauro & Davidzon, 2005; Kirby & Thorburn, 2008). More than 1000 nuclear genes encode proteins necessary for mitochondrial function that can explain the remaining cases (Human MitoCarta2.0). Among the 37 human aaRSs, mutations in mitochondrial and dual localized aaRS are associated with different organ involvements and could be responsible for a defect in mitochondrial protein synthesis (Diodato et al., 2014; Nafisinia et al., 2017; Sauter et al., 2015).

As no mitochondrial DNA mutations or deletion were detected in the patient presenting clinical manifestations compatible with a mitochondrial defect, we performed whole exome sequencing and identified biallelic mutations in the *KARS* gene, with one novel mutation.

Sixteen biallelic *KARS* mutations are linked to a large spectrum of neurologic or neurosensorial diseases (Table 1). Mutations in this gene were initially described to be associated with a peripheral neuropathy (McLaughlin et al., 2010) and non syndromic hearing impairment (Santos-Cortez et al., 2013). More complex phenotypes were also reported, including clinical associations evocative of a mitochondrial disorder (Kohda et al., 2016; Lieber et al., 2013; McMillan et al., 2015; Murray et al., 2017; Verrigni et al., 2017; Zhou et al., 2017). Our patient presented with an overlapping phenotype

with those previously described with hearing loss, abnormal white matter, lactic acidosis, and combined enzymatic defects of respiratory chain complexes. Nevertheless she had an atypical presentation with a stable evolution until 28 years old and worsening clinical manifestations in few years. In addition, she had visual impairment with white matter anomalies of optic radiations and optic neuropathy not previously reported.

Impact of the identified KARS mutations

In higher eukaryotes at least nine aaRSs, including the cytoplasmic KARS isoform belong to the MSC complex with three accessory proteins (p18, p38 and p43) (Havrylenko & Mirande, 2015).

Among the two identified variants in *KARS* gene, the p.Pro228Leu mutation was previously described (Lieber et al., 2013) and a recent functional analysis was performed, showing defect in mitochondria translation (Ruzzenente et al., 2018). Here we show that this KARS-Pro228Leu is severely affected for aminoacylation *in vitro*. The Pro228 amino acid is localized in the anticodon-binding domain of KARS close to the P-S207 phosphorylation site essential for p38 interaction and association with the MSC (Ofir-Birin et al., 2013). The P-S207 form of KARS is released from the MCS and translocates to the nucleus where it is associated to transcriptional activities. Among the cellular functions of this P-S207 KARS, its role in the production of the second messenger Ap4A has already been studied in the eye in various conditions such as a biomarker for raised intra ocular pressure in glaucoma were higher levels of Ap4A were observed as well as in the tears from patients suffering of other ocular pathologies, as dry eye and congenital aniridia (Castany et al., 2011; Guzman-Aranguez et al., 2007; Peral et al., 2006; Peral et al., 2015). The potential therapeutic

effects of dinucleotide polyphosphates have been proposed for various eye conditions including regulation of intra ocular pressure in a mouse model (Carracedo et al., 2016; Crooke et al., 2017). In this respect, it is interesting to underline that our patient presented with a non glaucomatous optic neuropathy developed in the context of a down regulation of KARS effectors suggesting that Ap4A supplementation could have been protective if Ap4A deficiency had been proven. This points to the probably subtle equilibrium of the Ap4A intraocular levels in various eye conditions (ie: glaucomatous versus non glaucomatous ganglion cell loss) as well as to the complex pathogenesis underlying these conditions. The known link of P-207 KARS regulating *MITF*, a gene mutated in Waardenburg syndrome type 2 and Tietze syndrome for which neurosensory hearing loss is well described, is also highly interesting as our patient first clinical manifestation was deafness pointing here to a link of this condition with this pathway. The p.Phe291Val mutation is a novel variant that hits the catalytic domain of the enzyme and affects an amino acid residue highly conserved among diverse metazoan species (Figure 3D) (http://misynpat.org) (Moulinier et al., 2017). The Phe291 amino acid is at the KARS-p38 interaction interface (Figure 3E). The KARS-Phe291Val variant has a 2-fold decrease in relative aminoacylation activity compared to wild type KARS.

The study of the expression level of both KARS isoforms (cytoplasmic and mitochondrial) was not performed for the other human *KARS* mutations previously reported. To better understand the disease mechanism of the mutations identified in our patient, we studied the impact of both mutations in the two KARS isoforms. Investigations on skin fibroblasts of the patient showed that both KARS isoforms are present at the mRNA level and that the mutations do not affect the splicing. Interestingly, we observed a similar level of cytoplasmic KARS mRNA in the patient

and control cells, whereas the cytoplasmic KARS protein level was decreased due to higher degradation or decreased stability of the mutant proteins, which could be due to lack of association to the MSC complex. Indeed, by using the yeast-two hybrid assay, we demonstrated that both mutations are associated with a significantly reduced interaction between cytoplasmic KARS and the core protein p38 of the MSC complex. These data were confirmed by coimmunoprecipitation assays on lysates from patient fibroblasts, showing that less KARS proteins were interacting with p38 compared to the control. In parallel to these effects on the cytoplasmic isoform of KARS, we observed an increase in mitochondrial KARS at the mRNA level and to some extent at the protein level. These results suggest that more mitochondrial KARS could be imported into the mitochondria and transformed into its active form. However, this cannot compensate for the lysine incorporation during the cytoplasmic production of respiratory chain proteins encoded by the nuclear genome, leading to the reduced level of cytochrome C oxidase COX4 subunit and to the partial decrease of complex I and IV activity in the skeletal muscle of the patient. A similar combined complex deficiency and reduction of cytochrome C oxidase was already reported for other patients with *KARS* mutations (Kohda et al., 2016; Verrigni et al., 2017).

In conclusion, we report biallelic mutations in the *KARS* gene, one of which had not been previously reported, in a patient presenting cerebellar ataxia and optic neuropathy in addition to the sensory deafness and neurological features already described. Our results show the implication of both mutations in the phenotype of the patient. However, further studies are needed to investigate more in details which proteins of the respiratory chain are affected and to what extent.

Availability of data and material

Data generated or analyzed during this study are included in the published article and the corresponding supplementary data. The raw sequencing data generated in the course of this study are not publicly available due to the protocol and the corresponding consents used that did not include such information. KARS' variants have been submitted to ClinVar with the following accession numbers SCV000808060 and SCV000808061 (https://www.ncbi.nlm.nih.gov/clinvar/). Anonymized NGS data and genomic variant data files will be made available upon request from qualified investigators studying the molecular basis of genomic disorders. Datasets can be obtained via the corresponding author on reasonable request.

Acknowledgments

We would like to thank the patient and her family for their participation. We thank Hubert Becker, Nina Entelis, Marie Sissler and Ivan Tarassov (MitoCross Labex, Université de Strasbourg, France) and Luc Moulinier (iCUBE, Strasbourg, France) for providing reagents and for discussions. We thank Agnès Rötig and Metodi Metodiev (Imagine Institute, Paris, France) for antibodies and for helpful discussions. The computing resources for this work were provided by the BICS and BISTRO bioinformatics platforms in Strasbourg.

Conflict of Interest

We declare no competing interests.

References

Adzhubei, I. A., Schmidt, S., Peshkin, L., Ramensky, V. E., Gerasimova, A., Bork, P., . . . Sunyaev, S. R. (2010). A method and server for predicting damaging missense mutations. *Nat Methods, 7*(4), 248-249. doi:10.1038/nmeth0410-248

Antonellis, A., & Green, E. D. (2008). The role of aminoacyl-tRNA synthetases in genetic diseases. *Annu Rev Genomics Hum Genet, 9*, 87-107. doi:10.1146/annurev.genom.9.081307.164204

Backenroth, D., Homsy, J., Murillo, L. R., Glessner, J., Lin, E., Brueckner, M., . . . Shen, Y. (2014). CANOES: detecting rare copy number variants from whole exome sequencing data. *Nucleic Acids Res, 42*(12), e97. doi:10.1093/nar/gku345

Bonnefond, L., Fender, A., Rudinger-Thirion, J., Giege, R., Florentz, C., & Sissler, M. (2005). Toward the full set of human mitochondrial aminoacyl-tRNA synthetases: characterization of AspRS and TyrRS. *Biochemistry, 44*(12), 4805-4816. doi:10.1021/bi047527z

Bourges, I., Ramus, C., Mousson de Camaret, B., Beugnot, R., Remacle, C., Cardol, P., . . . Issartel, J. P. (2004). Structural organization of mitochondrial human complex I: role of the ND4 and ND5 mitochondria-encoded subunits and interaction with prohibitin. *Biochem J, 383*(Pt. 3), 491-499. doi:10.1042/BJ20040256

Carracedo, G., Crooke, A., Guzman-Aranguez, A., Perez de Lara, M. J., Martin-Gil, A., & Pintor, J. (2016). The role of dinucleoside polyphosphates on the ocular surface and other eye structures. *Prog Retin Eye Res, 55*, 182-205. doi:10.1016/j.preteyeres.2016.07.001

Castany, M., Jordi, I., Catala, J., Gual, A., Morales, M., Gasull, X., & Pintor, J. (2011). Glaucoma patients present increased levels of diadenosine tetraphosphate, Ap(4)A, in the aqueous humour. *Exp Eye Res, 92*(3), 221-226. doi:10.1016/j.exer.2010.12.004

Crooke, A., Guzman-Aranguez, A., Carracedo, G., de Lara, M. J. P., & Pintor, J. (2017). Understanding the Presence and Roles of Ap4A (Diadenosine Tetraphosphate) in the Eye. *J Ocul Pharmacol Ther, 33*(6), 426-434. doi:10.1089/jop.2016.0146

Debard, S., Bader, G., De Craene, J. O., Enkler, L., Bar, S., Laporte, D., . . . Becker, H. D. (2017). Nonconventional localizations of cytosolic aminoacyl-tRNA synthetases in yeast and human cells. *Methods, 113*, 91-104. doi:10.1016/j.ymeth.2016.09.017

Dias, J., Octobre, G., Kobbi, L., Comisso, M., Flisiak, S., & Mirande, M. (2012). Activation of human mitochondrial lysyl-tRNA synthetase upon maturation of its premitochondrial precursor. *Biochemistry, 51*(4), 909-916. doi:10.1021/bi201337b

Dimauro, S., & Davidzon, G. (2005). Mitochondrial DNA and disease. *Ann Med, 37*(3), 222-232. doi:10.1080/07853890510007368

Diodato, D., Ghezzi, D., & Tiranti, V. (2014). The Mitochondrial Aminoacyl tRNA Synthetases: Genes and Syndromes. *Int J Cell Biol, 2014*, 787956. doi:10.1155/2014/787956

Fonseca, B., Martinez-Aguila, A., de Lara, M. J. P., & Pintor, J. (2017). Diadenosine tetraphosphate as a potential therapeutic nucleotide to treat glaucoma. *Purinergic Signal, 13*(2), 171-177. doi:10.1007/s11302-016-9547-y

Francin, M., Kaminska, M., Kerjan, P., & Mirande, M. (2002). The N-terminal domain of mammalian Lysyl-tRNA synthetase is a functional tRNA-binding domain. *J Biol Chem, 277*(3), 1762-1769. doi:10.1074/jbc.M109759200

Genomes Project, C., Auton, A., Brooks, L. D., Durbin, R. M., Garrison, E. P., Kang, H. M., . . . Abecasis, G. R. (2015). A global reference for human genetic variation. *Nature, 526*(7571), 68-74. doi:10.1038/nature15393

Geoffroy, V., Herenger, Y., Kress, A., Stoetzel, C., Piton, A., Dollfus, H., & Muller, J. (2018). AnnotSV: An integrated tool for Structural Variations annotation. *Bioinformatics*. doi:10.1093/bioinformatics/bty304

Geoffroy, V., Pizot, C., Redin, C., Piton, A., Vasli, N., Stoetzel, C., . . . Muller, J. (2015). VaRank: a simple and powerful tool for ranking genetic variants. *PeerJ, 3*, e796. doi:10.7717/peerj.796

Gietz, R. D., Triggs-Raine, B., Robbins, A., Graham, K. C., & Woods, R. A. (1997). Identification of proteins that interact with a protein of interest: applications of the yeast two-hybrid system. *Mol Cell Biochem, 172*(1-2), 67-79.

Golemis, E. A., Serebriiskii, I., Finley, R. L., Jr., Kolonin, M. G., Gyuris, J., & Brent, R. (2001). Interaction trap/two-hybrid system to identify interacting proteins. *Curr Protoc Cell Biol, Chapter 17*, Unit 17 13. doi:10.1002/0471143030.cb1703s08

Gotz, A., Tyynismaa, H., Euro, L., Ellonen, P., Hyotylainen, T., Ojala, T., . . . Suomalainen, A. (2011). Exome sequencing identifies mitochondrial alanyl-tRNA synthetase mutations in infantile mitochondrial cardiomyopathy. *Am J Hum Genet, 88*(5), 635-642. doi:10.1016/j.ajhg.2011.04.006

Guzman-Aranguez, A., Crooke, A., Peral, A., Hoyle, C. H., & Pintor, J. (2007). Dinucleoside polyphosphates in the eye: from physiology to therapeutics. *Prog Retin Eye Res, 26*(6), 674-687. doi:10.1016/j.preteyeres.2007.09.001

Havrylenko, S., & Mirande, M. (2015). Aminoacyl-tRNA synthetase complexes in evolution. *Int J Mol Sci, 16*(3), 6571-6594. doi:10.3390/ijms16036571

Kaminska, M., Havrylenko, S., Decottignies, P., Gillet, S., Le Marechal, P., Negrutskii, B., & Mirande, M. (2009). Dissection of the structural organization of the aminoacyl-tRNA synthetase complex. *J Biol Chem, 284*(10), 6053-6060. doi:10.1074/jbc.M809636200

Kaminska, M., Shalak, V., Francin, M., & Mirande, M. (2007). Viral hijacking of mitochondrial lysyl-tRNA synthetase. *J Virol, 81*(1), 68-73. doi:10.1128/JVI.01267-06

Kao, S. H., Wang, W. L., Chen, C. Y., Chang, Y. L., Wu, Y. Y., Wang, Y. T., . . . Yang, P. C. (2015). Analysis of Protein Stability by the Cycloheximide Chase Assay. *Bio Protoc, 5*(1). doi:10.21769/BioProtoc.1374

Kirby, D. M., & Thorburn, D. R. (2008). Approaches to finding the molecular basis of mitochondrial oxidative phosphorylation disorders. *Twin Res Hum Genet, 11*(4), 395-411. doi:10.1375/twin.11.4.395

Kohda, M., Tokuzawa, Y., Kishita, Y., Nyuzuki, H., Moriyama, Y., Mizuno, Y., . . . Okazaki, Y. (2016). A Comprehensive Genomic Analysis Reveals the Genetic Landscape of Mitochondrial Respiratory Chain Complex Deficiencies. *PLoS Genet, 12*(1), e1005679. doi:10.1371/journal.pgen.1005679

Kumar, P., Henikoff, S., & Ng, P. C. (2009). Predicting the effects of coding non-synonymous variants on protein function using the SIFT algorithm. *Nat Protoc, 4*(7), 1073-1081. doi:10.1038/nprot.2009.86

Ladner, C. L., Yang, J., Turner, R. J., & Edwards, R. A. (2004). Visible fluorescent detection of proteins in polyacrylamide gels without staining. *Anal Biochem, 326*(1), 13-20. doi:10.1016/j.ab.2003.10.047

Latour, P., Thauvin-Robinet, C., Baudelet-Mery, C., Soichot, P., Cusin, V., Faivre, L., . . . Rousson, R. (2010). A major determinant for binding and aminoacylation of tRNA(Ala) in cytoplasmic Alanyl-tRNA synthetase is mutated in dominant axonal Charcot-Marie-Tooth disease. *Am J Hum Genet, 86*(1), 77-82. doi:10.1016/j.ajhg.2009.12.005

Lee, Y. N., Nechushtan, H., Figov, N., & Razin, E. (2004). The function of lysyl-tRNA synthetase and Ap4A as signaling regulators of MITF activity in FcepsilonRI-activated mast cells. *Immunity, 20*(2), 145-151.

Lek, M., Karczewski, K. J., Minikel, E. V., Samocha, K. E., Banks, E., Fennell, T., . . . Exome Aggregation, C. (2016). Analysis of protein-coding genetic variation in 60,706 humans. *Nature, 536*(7616), 285-291. doi:10.1038/nature19057

Lieber, D. S., Calvo, S. E., Shanahan, K., Slate, N. G., Liu, S., Hershman, S. G., . . . Mootha, V. K. (2013). Targeted exome sequencing of suspected mitochondrial disorders. *Neurology, 80*(19), 1762-1770. doi:10.1212/WNL.0b013e3182918c40

McLaughlin, H. M., Sakaguchi, R., Liu, C., Igarashi, T., Pehlivan, D., Chu, K., . . . Antonellis, A. (2010). Compound heterozygosity for loss-of-function lysyl-tRNA synthetase mutations in a patient with peripheral neuropathy. *Am J Hum Genet, 87*(4), 560-566. doi:10.1016/j.ajhg.2010.09.008

McMillan, H. J., Humphreys, P., Smith, A., Schwartzentruber, J., Chakraborty, P., Bulman, D. E., . . . Geraghty, M. T. (2015). Congenital Visual Impairment and Progressive Microcephaly Due to Lysyl-Transfer Ribonucleic Acid (RNA)

Synthetase (KARS) Mutations: The Expanding Phenotype of Aminoacyl-Transfer RNA Synthetase Mutations in Human Disease. *J Child Neurol, 30*(8), 1037-1043. doi:10.1177/0883073814553272

Mirande, M., Cirakoglu, B., & Waller, J. P. (1982). Macromolecular complexes from sheep and rabbit containing seven aminoacyl-tRNA synthetases. III. Assignment of aminoacyl-tRNA synthetase activities to the polypeptide components of the complexes. *J Biol Chem, 257*(18), 11056-11063.

Moulinier, L., Ripp, R., Castillo, G., Poch, O., & Sissler, M. (2017). MiSynPat: An integrated knowledge base linking clinical, genetic, and structural data for disease-causing mutations in human mitochondrial aminoacyl-tRNA synthetases. *Hum Mutat, 38*(10), 1316-1324. doi:10.1002/humu.23277

Murray, C. R., Abel, S. N., McClure, M. B., Foster, J., 2nd, Walke, M. I., Jayakar, P., . . . Tekin, M. (2017). Novel Causative Variants in DYRK1A, KARS, and KAT6A Associated with Intellectual Disability and Additional Phenotypic Features. *J Pediatr Genet, 6*(2), 77-83. doi:10.1055/s-0037-1598639

Nafisinia, M., Riley, L. G., Gold, W. A., Bhattacharya, K., Broderick, C. R., Thorburn, D. R., . . . Christodoulou, J. (2017). Compound heterozygous mutations in glycyl-tRNA synthetase (GARS) cause mitochondrial respiratory chain dysfunction. *PLoS One, 12*(6), e0178125. doi:10.1371/journal.pone.0178125

Ofir-Birin, Y., Fang, P., Bennett, S. P., Zhang, H. M., Wang, J., Rachmin, I., . . . Guo, M. (2013). Structural switch of lysyl-tRNA synthetase between translation and transcription. *Mol Cell, 49*(1), 30-42. doi:10.1016/j.molcel.2012.10.010

Peral, A., Carracedo, G., Acosta, M. C., Gallar, J., & Pintor, J. (2006). Increased levels of diadenosine polyphosphates in dry eye. *Invest Ophthalmol Vis Sci, 47*(9), 4053-4058. doi:10.1167/iovs.05-0980

Peral, A., Carracedo, G., & Pintor, J. (2015). Diadenosine polyphosphates in the tears of aniridia patients. *Acta Ophthalmol, 93*(5), e337-342. doi:10.1111/aos.12626

Quevillon, S., Robinson, J. C., Berthonneau, E., Siatecka, M., & Mirande, M. (1999). Macromolecular assemblage of aminoacyl-tRNA synthetases: identification of protein-protein interactions and characterization of a core protein. *J Mol Biol, 285*(1), 183-195. doi:10.1006/jmbi.1998.2316

Reese, M. G., Eeckman, F. H., Kulp, D., & Haussler, D. (1997). Improved splice site detection in Genie. *J Comput Biol, 4*(3), 311-323.

Ruzzenente, B., Assouline, Z., Barcia, G., Rio, M., Boddaert, N., Munnich, A., . . . Metodiev, M. D. (2018). Inhibition of mitochondrial translation in fibroblasts from a patient expressing the KARS p.(Pro228Leu) variant and presenting with sensorineural deafness, developmental delay, and lactic acidosis. *Hum Mutat, 39*(12), 2047-2059. doi:10.1002/humu.23657

Santos-Cortez, R. L., Lee, K., Azeem, Z., Antonellis, P. J., Pollock, L. M., Khan, S., . . . Leal, S. M. (2013). Mutations in KARS, encoding lysyl-tRNA synthetase,

cause autosomal-recessive nonsyndromic hearing impairment DFNB89. *Am J Hum Genet, 93*(1), 132-140. doi:10.1016/j.ajhg.2013.05.018

Sauter, C., Lorber, B., Gaudry, A., Karim, L., Schwenzer, H., Wien, F., . . . Sissler, M. (2015). Neurodegenerative disease-associated mutants of a human mitochondrial aminoacyl-tRNA synthetase present individual molecular signatures. *Sci Rep, 5*, 17332. doi:10.1038/srep17332

Shapiro, M. B., & Senapathy, P. (1987). RNA splice junctions of different classes of eukaryotes: sequence statistics and functional implications in gene expression. *Nucleic Acids Res, 15*(17), 7155-7174.

Sherry, S. T., Ward, M. H., Kholodov, M., Baker, J., Phan, L., Smigielski, E. M., & Sirotkin, K. (2001). dbSNP: the NCBI database of genetic variation. *Nucleic Acids Res, 29*(1), 308-311.

Sofou, K., Kollberg, G., Holmstrom, M., Davila, M., Darin, N., Gustafsson, C. M., . . . Asin-Cayuela, J. (2015). Whole exome sequencing reveals mutations in NARS2 and PARS2, encoding the mitochondrial asparaginyl-tRNA synthetase and prolyl-tRNA synthetase, in patients with Alpers syndrome. *Mol Genet Genomic Med, 3*(1), 59-68. doi:10.1002/mgg3.115

Tolkunova, E., Park, H., Xia, J., King, M. P., & Davidson, E. (2000). The human lysyl-tRNA synthetase gene encodes both the cytoplasmic and mitochondrial enzymes by means of an unusual alternative splicing of the primary transcript. *J Biol Chem, 275*(45), 35063-35069. doi:10.1074/jbc.M006265200

Verrigni, D., Diodato, D., Di Nottia, M., Torraco, A., Bellacchio, E., Rizza, T., . . . Carrozzo, R. (2017). Novel mutations in KARS cause hypertrophic cardiomyopathy and combined mitochondrial respiratory chain defect. *Clin Genet, 91*(6), 918-923. doi:10.1111/cge.12931

Waterhouse, A. M., Procter, J. B., Martin, D. M., Clamp, M., & Barton, G. J. (2009). Jalview Version 2--a multiple sequence alignment editor and analysis workbench. *Bioinformatics, 25*(9), 1189-1191. doi:10.1093/bioinformatics/btp033

Yeo, G., & Burge, C. B. (2004). Maximum entropy modeling of short sequence motifs with applications to RNA splicing signals. *J Comput Biol, 11*(2-3), 377-394. doi:10.1089/1066527041410418

Zhou, X. L., He, L. X., Yu, L. J., Wang, Y., Wang, X. J., Wang, E. D., & Yang, T. (2017). Mutations in KARS cause early-onset hearing loss and leukoencephalopathy: Potential pathogenic mechanism. *Hum Mutat, 38*(12), 1740-1750. doi:10.1002/humu.23335

Figures

Figure 1: **Fundus photograph and Brain MRI of the patient** A) Fundus photographs of the patient showing optic neuropathy with symmetric temporal wedges of disc pallor. B) Brain MRI: axial FLAIR weighted images (a-c), axial diffusion weighted images (d-f) and Apparent Diffusion Coefficient maps (g-i) : Hyperintense FLAIR (a-c) lesions of both dentate nucleus (arrow), optic radiations (arrow head) and of the corpus callosum splenium (cross). The lesions are heterogeneous on diffusion weighted images (d-f), with mild hyperintense areas (circle) (d-f) corresponding to elevated diffusion coefficient on Apparent Diffusion Coefficient maps (circle) (g-i) and more hyperintense areas (star) (d-f) corresponding to restricted diffusion coefficient on Apparent Diffusion Coefficient maps (star) (g-i).

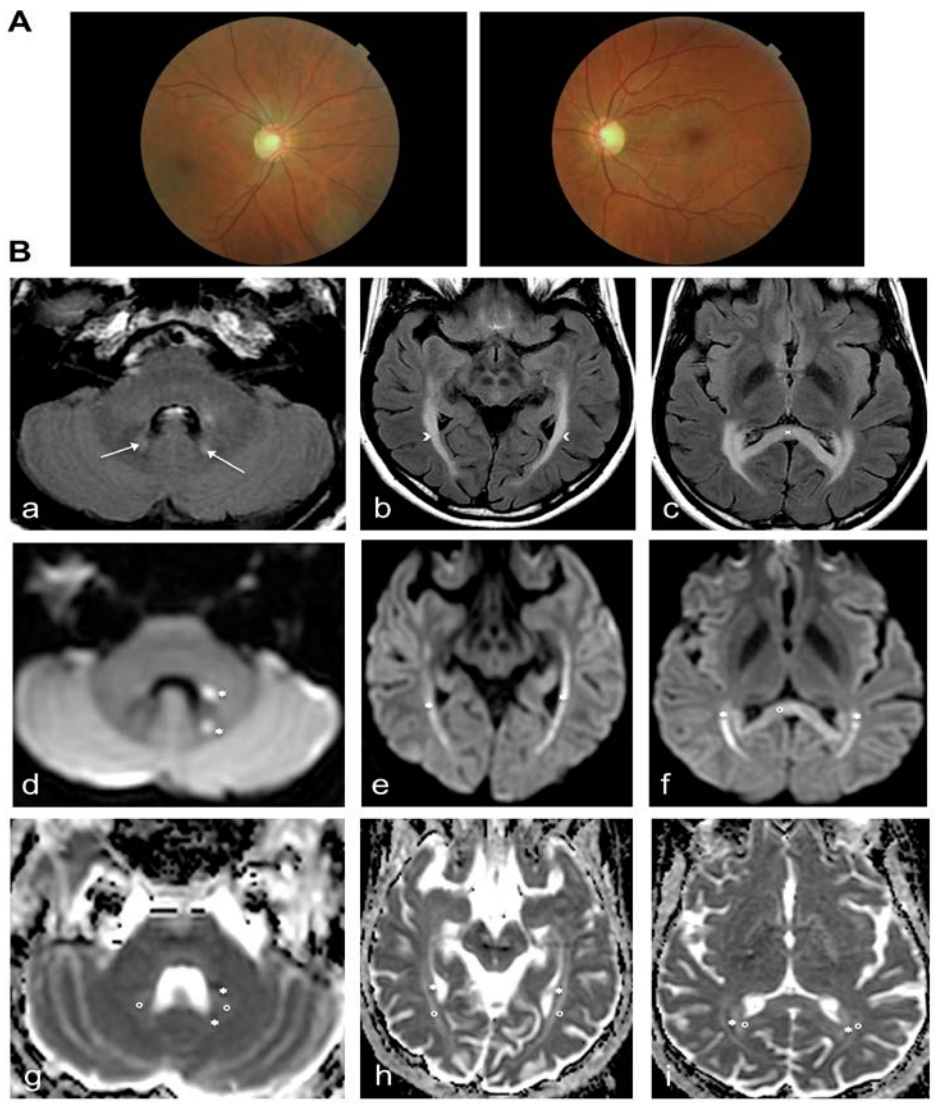

Figure 2: **Morphologic and enzymatic analyses on muscle biopsy of the patient** A) No ragged-red fibers were observed on modified Gomori trichrome staining (a), but numerous COX negative fibers were present (star). Scale bar 50 µm. B) Activity of the respiratory chain complexes (normalized to citrate synthase activity), showing partial deficit of complex I (68% of the reference range mean) and complex IV (62%). Abnormal activity ratios confirm imbalance of complexes.

A

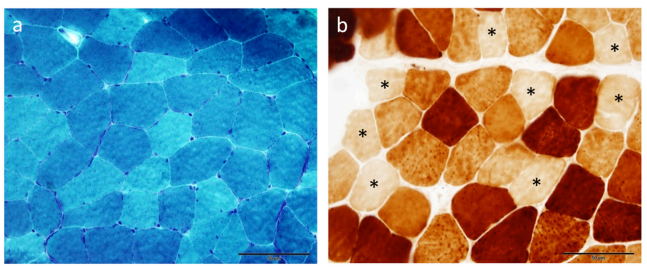

B

	Enzyme activity (nmoles/min/mg)	
	Patient	Reference range
CI	9.7 (68%)	14.3 (9.7-19.7)
CII	20.2	16.1 (12.7-21.4)
CIII	95	115.8 (79.9-140.6)
CIV	54.2 (62%)	87.7 (71-116.7)
Citrate synthase	74.1	180.7 (89.6-334)
Succinate déshydrogenase	4.7	6.9 (5.5-9)
Succinate cytochrome c reductase CII and CIII	6.9	6.5 (4.6-9.8)

	Enzyme activity ratio	
	Patient	Reference range
Ratio IV/II+III	7.79	13.7+/-3.7 (8.5-21.1)
Ratio I/II+III	1.4	2.3+/-0,58 (1.56-4.01)
Ratio I/III	0.1	0.13+/-0,02 (0.09-0.16)
Ratio I/IV	0.18	0.17+/-0,03 (0.13-0.21)
Ratio III/IV	1.75	1.39+/-0,24 (0.93-1.95)
Ratio III/II+III	13.67	18.5+/-4,1 (12.4-27.1)
Ratio II/IV	0.37	0.19+/-0,05 (0.13-0.27)

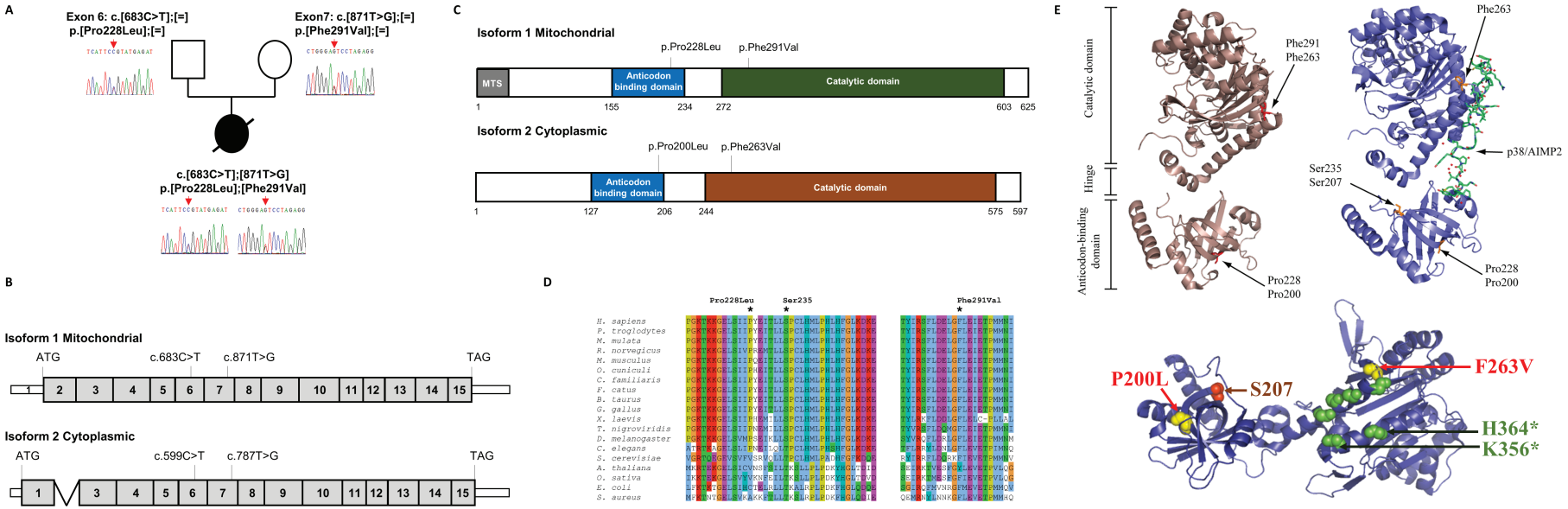

Figure 3: **Mutations in *KARS* gene identified in the patient** A) The family pedigree with the affected individual harboring two biallelic mutations in *KARS*. The segregation analysis confirmed autosomal-recessive inheritance. The *KARS* mutations are indicated by arrows. Squares, males; circle, female; black symbol, individual affected B) Schematic representation of the two isoforms of *KARS* cDNA and the mutations reported in our patient. C) Schematic representation of the two isoforms of KARS protein and the main domains (in blue and orange) including the mitochondria targeting sequence (MTS) and the *KARS* mutations reported in our patient. D) Multi-species sequence alignment of the hLysRS protein showing the evolutionary conservation of the two mutated amino acids (Pro228Leu and Phe291Val) and the Ser235 amino acid. The alignment is shown thanks to Jalview (Waterhouse, Procter, Martin, Clamp, & Barton, 2009). E) The crystal structure of the KARS-p38 complex (PDB 4dpg) was loaded into PyMOL. B. The aminoacid residues Pro200 and Phe263 affected by the patient mutations and the Ser207 phosphorylation site regulating KARS interaction with p38 are indicated on the KARS and KARS-p38/AIMP2 complex.

Figure 4: **Expression of KARS at mRNA and protein level, from skin fibroblasts of the patient** A) cDNA sequence after amplification from exon 5 to 9 (using primers 5F and 9R) showing the two mutations. B) Quantification of KARS mRNA showed an increased amount of mitochondrial KARS mRNA in the patient compared to controls. C) Expression of mitochondrial and cytoplasmic forms of KARS proteins in control (ctrl) and patient (affected) fibroblasts observed by western blot. KARS was detected with three different antibodies recognizing either both isoforms of KARS when directed against the catalytic domain (total) or specifically the cytoplasmic or mitochondrial isoforms. The asterisk indicates the band at the right size. The stainfree loading control shows the total amount of proteins loaded on the gel and was used for quantification. Quantification of total, cytoplasmic (cyto) and mitochondrial (mito) isoforms of KARS in patient cells as detected with the three antibodies mentioned above and represented as percentage (%) of the amount of KARS in control cells (ctrl). Values are the mean of five experiments. Statistical analyses were done with the T-Test and the p-values were determined, *: p< 0,05, ** p<0,01. D) Control (ctrl) and patient (affected) cells were incubated with cycloheximide (100 mg/L) for 0 to 8 hours before being collected and anti- KARS western blot was performed on the cell lysates. The total protein level of KARS was determined relative to the house keeping protein GAPDH used as loading control.

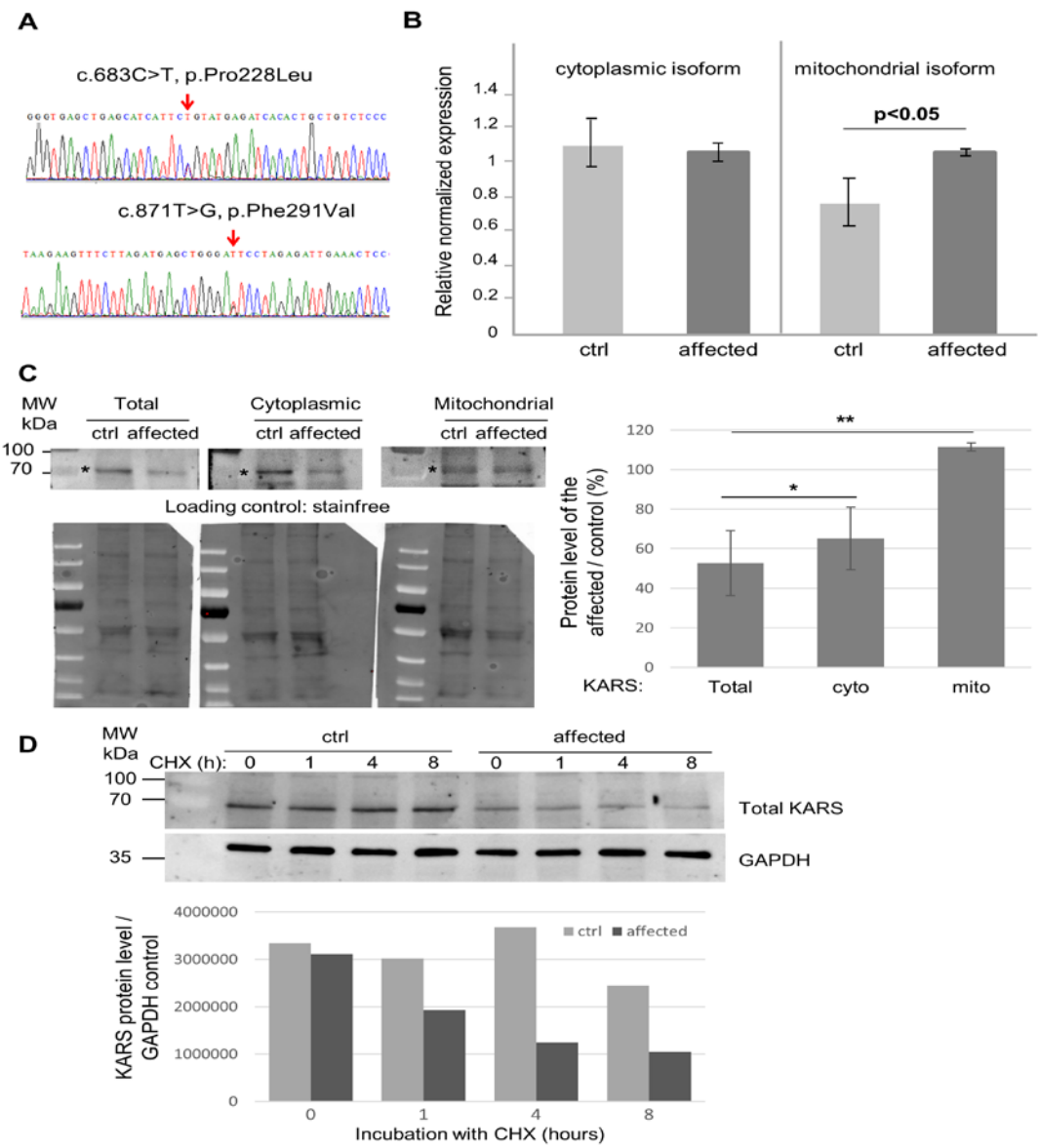

Figure 5: **Immunofluorescence on patient's skin fibroblasts** A decreased amount of cytoplasmic KARS was observed in patient (affected) fibroblasts compared to control (ctrl) by anti-KARS immunofluorescence microscopy. Cells were grown on coverslips, stained with mitotracker red and observed under a fluorescence microscope after anti-KARS antibodies labeling. The immunofluorescence staining shows mostly the cytoplasmic KARS proteins in control fibroblasts and a decreased fluorescence staining was observed in the patient cells. Images were taken with a 400X magnification, scale bar 5 µm.

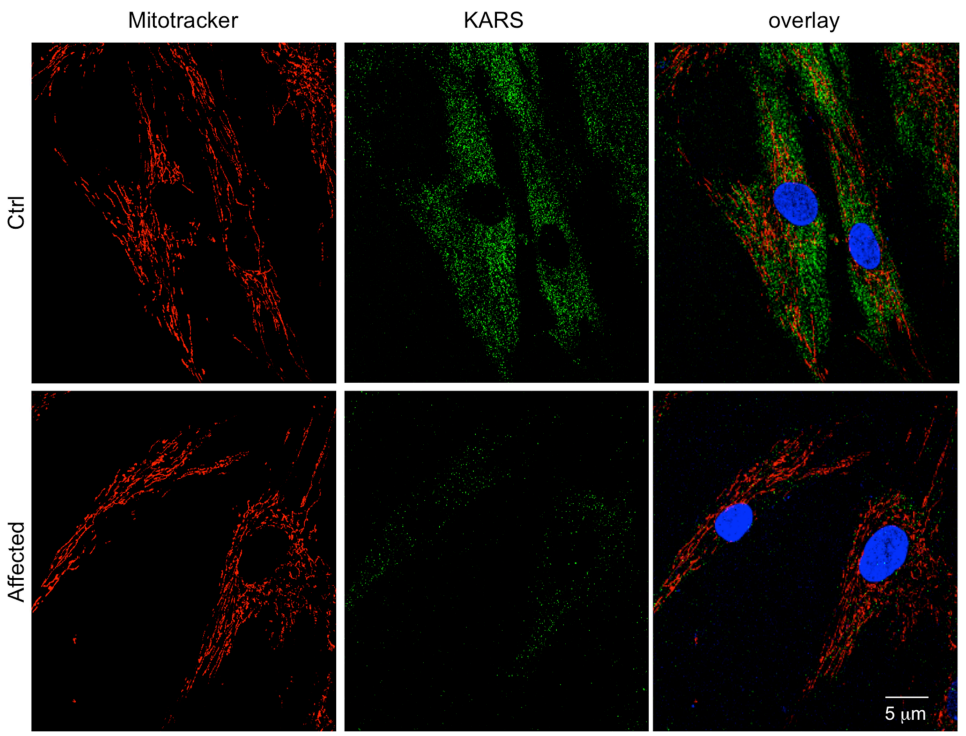

Figure 6: **The mutant KARS proteins show decreased interaction with p38** A) The EGY48 yeast cells bearing the pSH18-34 LacZ reporter plasmid were transformed by pEG202 plasmid expressing p38, KARS, KARS-P200L or KARS-F263V cDNA in fusion with the LexA DNA-binding protein, and there was no production of β-galactosidase, showing that there is no self-activation. The EGY48 yeast cells bearing the pJK101 control plasmid were transformed by pEG202 plasmid expressing p38, KARS, KARS-P200L or KARS-F263V cDNA, and expression of the LexA fusions was confirmed by this repression assay. The EGY48 yeast cells bearing the pSH18-34 LacZ reporter and pEG202-LexA plasmids were transformed by pJG4-5 plasmid expressing p38, KARS, KARS-P200L or KARS-F263V cDNA in fusion with the *GAL1* promoter transcriptional activation domain; no β-galactosidase activity was observed showing that there is no self-DNA binding. B) The two-hybrid interaction assay was done in EGY48 yeast cells bearing the pSH18-34 LacZ reporter transformed by pEG202-p38 or pJG4-5-p38 and by pJG4-5- or pEG202-KARS, -KARS-P200L or -KARS-F263V plasmid respectively, and the β-galactosidase activity was determined by the ONPG colorimetric assay measuring the optical density (OD) at 420 nm that corresponds to ONP production. The KARS missense mutations impair interaction with p38. Statistical analyses were done with the T-Test and the p-values were determined, ***: $p<0{,}005$. C) Coimmunoprecipitation (Co-IP) between p38 and KARS, done in primary human fibroblasts. Control (ctrl) or patient (affected) fibroblasts were collected and lysed in non-denaturing lysis buffer. Immunoprecipitation was performed on the total whole lysates using antibodies directed against KARS (Co-IP KARS) or p38 (Co-IP p38), or without antibodies (Neg-IP) as a control. Proteins were detected by western blot in the whole cell lysates (Input) and the immunoprecipitations (neg-IP, Co-IP KARS and Co-IP p38) using the KARS and p38 antibodies. Actin B (ACTB) was used as a negative control.

A

	Self - activation	LexA fusion expression	Self-DNA binding
KARS	-	+	-
KARS-P200L	-	+	-
KARS-F263V	-	+	-

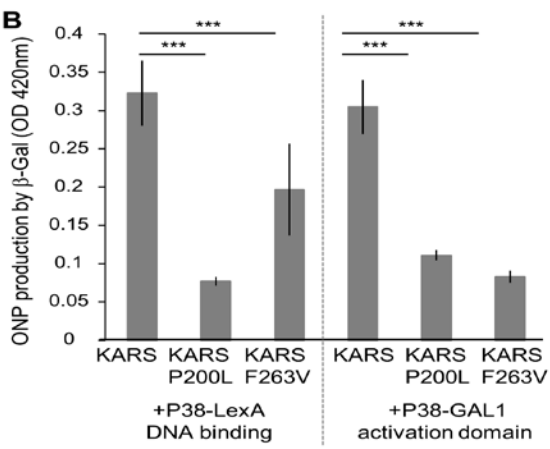

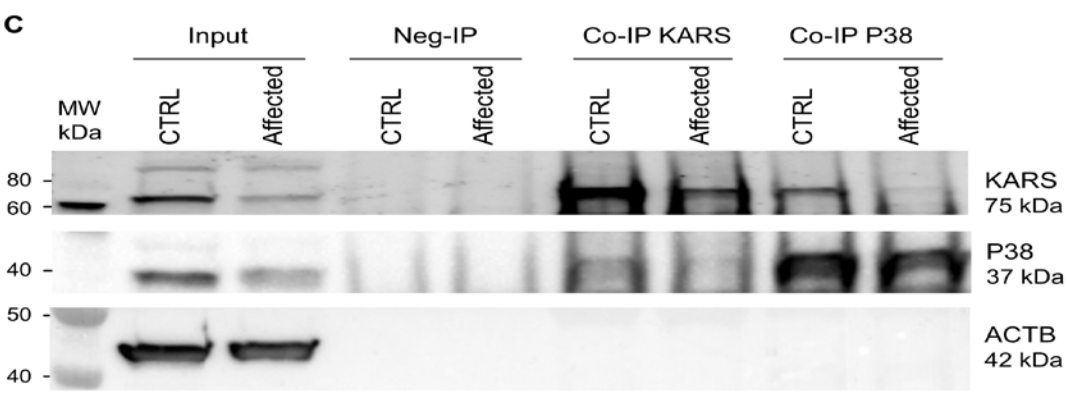

Figure 7: **KARS variants display decreased aminoacylation efficiency and impact synthesis of lysine-rich nuclear encoded mitochondrial proteins.** A) Time course of aminoacylation by KARS wild type and the two variants. Aminoacylations were performed with 10 nM of enzyme (KARS, KARS-P200L or KARS-F263V, as indicated), 4 µM of total yeast tRNA and 0.5 µM of [^{3}H]-Lysine, the values are the mean of three experiments with standard deviation error bars. The relative catalytic activity of the variants compared to the wild type KARS is indicated. B) Expression of proteins from the mitochondrial chain in control (ctrl) and patient (affected) fibroblasts. Cells were harvested and western blot against GRIM19, COX4, NDUFB6 and COX2 performed. Content in lysine (K) as % of total number of amino acids indicated as well as whether the gene is in the nuclear or mitochondrial genome.

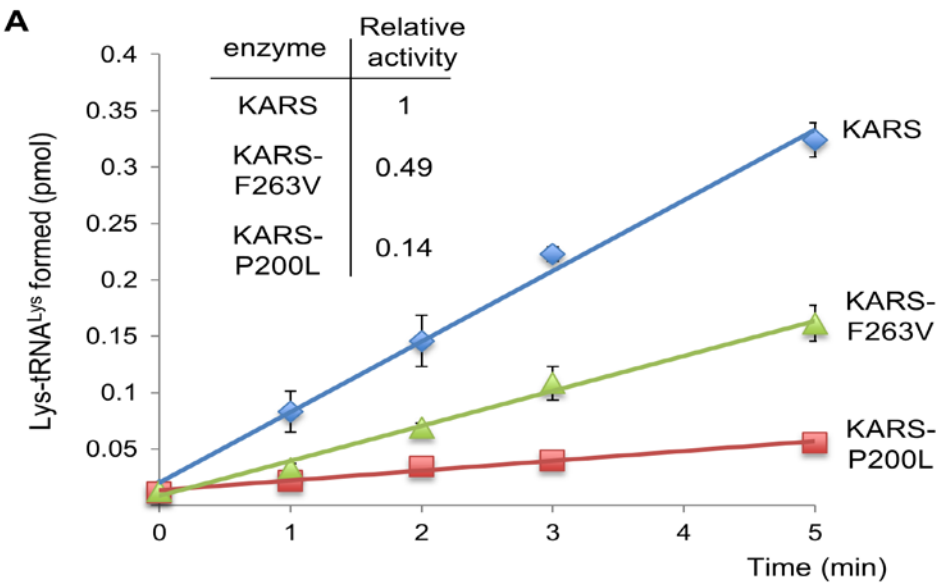

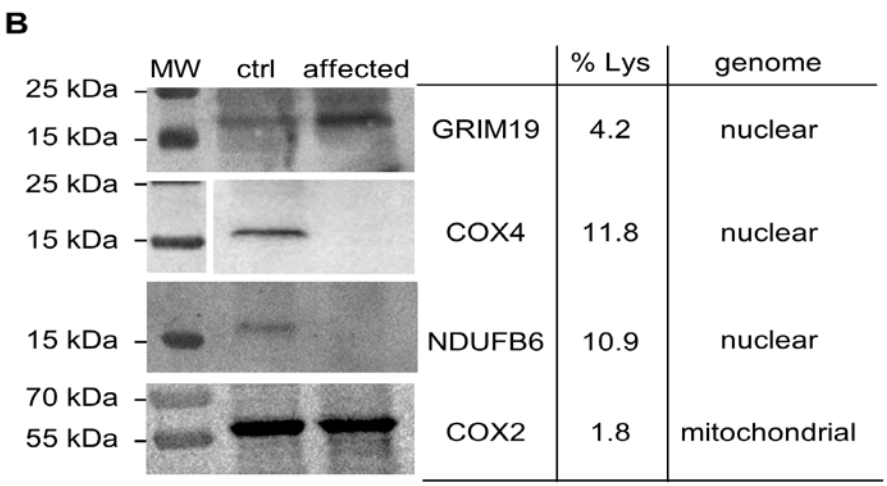

Tables

Table 1: Reported mutations in the *KARS* gene associated with the phenotypes (hmz: homozygous; htz: heterozygous; cmpdt htz: compound heterozygous).

	McLaughlin et *al.*, 2010	**Santos-Cortes et *al.*, 2013**	**Lieber et *al.*, 2013**	**McMillan et *al.*, 2014**	**Retterer et *al.*, 2016**	**Khoda et *al.*, 2016**	**Verrigni et *al.*, 2016**	**Chen et *al.*, 2016**	**Jung et *al.*, 2017**	**Zhou et *al.*, 2017**	**Murray et *al.*, 2017**
Number of patients	2 from 2 families	3 from 3 families	1	1	2	1	1	3	1	2 from one family	2 from one family
Microcephaly				+							+
Developmental delay	+ (1)		+	+			+			+	+
Peripheral neuropathy	+ (2)										
Other neurological features			+ (hypotonia, dystonia)	+ (seizures)	+		+ (myopathy)			+ (cognitive decline)	+ (hypotonia, seizures, ataxia)
Mitochondrial defect			Increased mtDNA in muscle			Combined complex deficiencies	Combined complex deficiencies				
Cerebral anomalies				+ (symmetric abnormal subcortical white matter, hypogenesis of corpus callosum)			normal			+ (symmetric signal anomalies in the frontal white matter periventricular and the corpus callosum)	CT (calcifications of the left occipitoparietal junction)
Hearing impairment		+	+					+	+	+	+
Ophthalmologic features			+ (strabismus, ophtalmoplegia)	+ (severe visual loss, pendular nystagmus)						normal	
Cardiomyopathy							+				
Other features	Vestibular Schwannoma, dysmorphic features (1)					Mitochondrial cytopathy					
Mutation in *KARS* gene NM_001130089.1	cmpdt htz : c.398T>A (p.L133H) c.524_525dupTT htz: c.906C>G (p.I302M)	hmz : c.517T>C (p.Y173H) hmz : c.1129G>A (p.D377N)	cmpdt htz : c.683C>T (p.P228L) c.1760C>T (p.T587M)	cmpdt htz : c.1396C>T (p.R466W) c.1657G>A (p.E553K)	htz: c.972G>A (p.M324I) htz: del ex 5-8	cmpdt htz : c.1037T>C (p.I346T) c.1427T>A (p.V476D)	cmpdt htz : c.1133T>A (p.L378H) c.1253C>G (p.P418R)	htz : c.1409G>T (p.R470M)	htz : c.1450T>G (p.C484G)	cmpdt htz : c.1430G>A (p.R477H) c.1513C>T (p.P505S)	c.1466T>G (p.F489C) c.1577C>T (p.A526V)